Expanded View Figures

Figure EV1. Isolation and verification of histone-humanized yeasts.

A Dual-plasmid histone shuffle assay overview. First, a strain with all core histone gene clusters deleted is maintained with a single set of yeast histone genes on the counter-selectable *URA3* plasmid (Haase *et al*, 2019). To shuffle out the yeast histones for human histones, a second plasmid encoding the four core human histones and with a *TRP1* selectable marker is transformed into the shuffle strain. The shuffle strains in then grown on media containing 5–FOA to force the cells to grow with exclusively human histones.

B Example humanization experiment results. Plates are shown at two time points to illustrate the severe growth defects upon the initial humanization event. Two colonies were isolated, one retaining all yeast histones (either through inactivation of *URA3* or some plasmid recombination event) and a *bona fide* histone-humanized clone as verified by PCR genotyping (Haase *et al*, 2019). Lanes 1–4, PCR genotyping of yeast H2A, H2B, H4, and H3, respectively; lanes 5–8 PCR genotyping of human H2A, H2B, H3, and H4, respectively.

C Whole genome sequencing coverage plots of the two histone plasmids (human histones, red; yeast histones, green) are shown for the parental shuffle strain prior to humanization and for histone-humanized clones (yHs9–yHs15). Box and whisker plot of the sliding window coverage for each plasmid from the indicated strain ($n = 1$), the central band represents the median coverage of all windows, the box extends from the 25th to 75th percentile, and the whiskers represent the 95% confidence interval.

D YPD plate growth assays for histone-humanized clones from the original unevolved glycerol stock and the evolved descendants after ~ 30 generations of growth. The scale bar represents 5 mm.

E Box and whisker plots of number of mutations observed per histone-humanized lineages. Each dot represents the number of mutations observed in a histone-humanized isolate (biological replicate, $n = 57$), the central band represents the median, the box extends from the 25th to 75th percentile, and the whiskers represent the minimum and maximum.

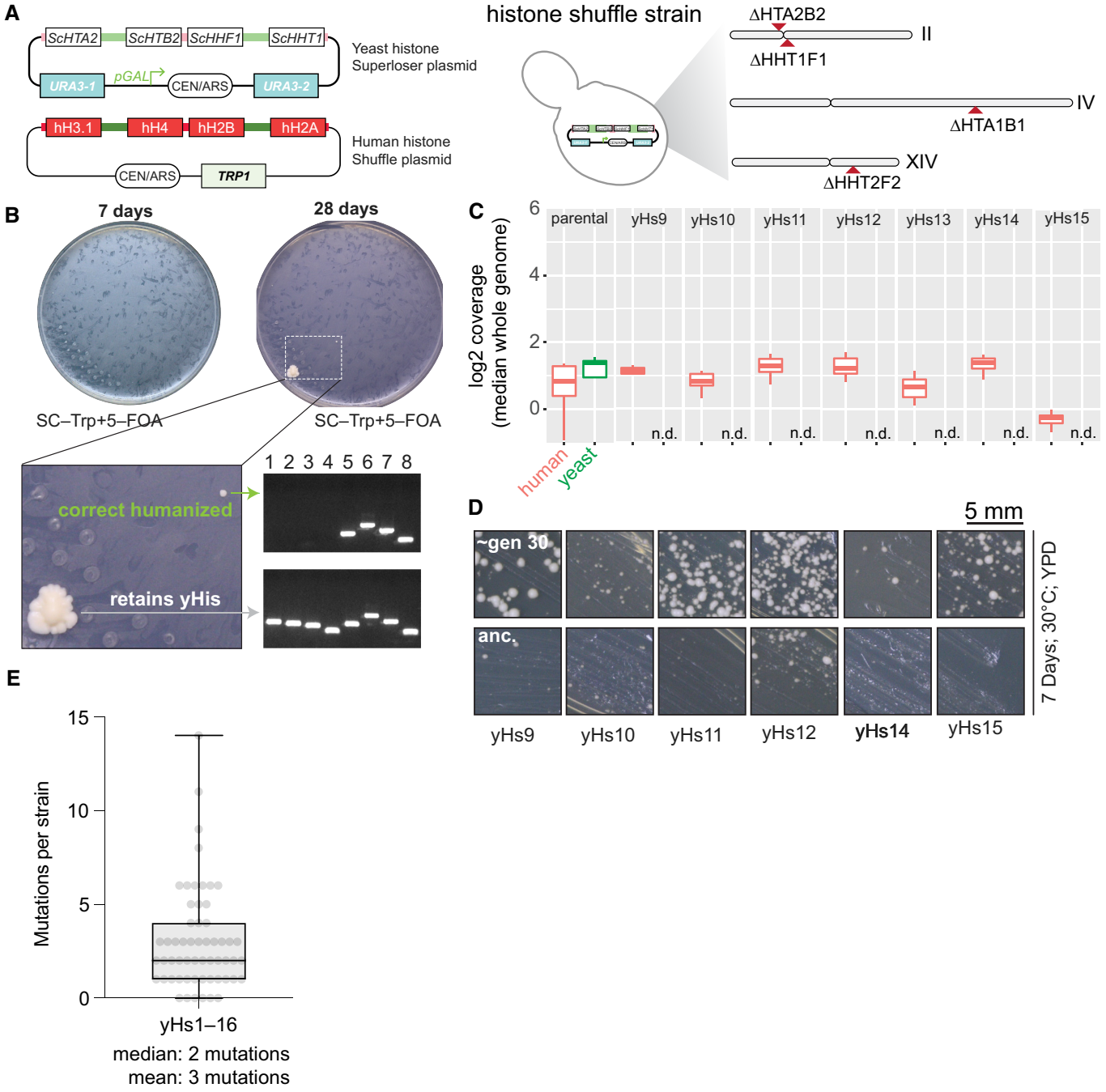

Figure EV1.

Figure EV2. CRISPR-Cas9 mediated mutation of outer kinetochore genes and suppression validation.

A Example CRISPR/Cas9 editing transformation to scarlessly introduce each point missense mutation to an isogenic histone shuffle strain. Note in the absence of dsDNA donor the sgRNA targeting *DAD1* results in a severe killing phenotype and upon co-transformation with a proper dsDNA, the killing phenotype is rescued.

B Example Sanger tracks for the edited $DAD1^{E50D}$ mutation and wild-type sequence. The targeting PAM is highlighted in blue, the edited codon in green, and the modified base pairs in red.

C Growth assay on rich medium (YPD) for the indicated histone shuffle strains with yeast histones. Spots are 10-fold serial dilutions from starting OD_{600} of 1.0.

D Example suppressor mutation sufficiency histone-humanization experiment is shown for the $DAD1^{E50D}$ mutation. Two concentrations of cells were plated (10^6 and 10^7 ml^{-1}).

E Histone humanizations for all tested suppressor mutations are shown. The average rates for wild-type strains are plotted as a gray-dashed line. Significance was determined with a Kruskal–Wallis test of the mean frequency of 5-FOA^R for each mutant versus the mean frequency of 5-FOA^R of wild type, with multiple-comparison corrections with the false discovery rate method. Green boxes represent suppressors who significantly increased the rate of humanization above wild-type level. Each dot represents a biological replicate of the histone humanization assay ($n \geq 4$), the central band represents the median, the box extends from the 25^{th} to 75^{th} percentile, and the whiskers represent the minimum and maximum.

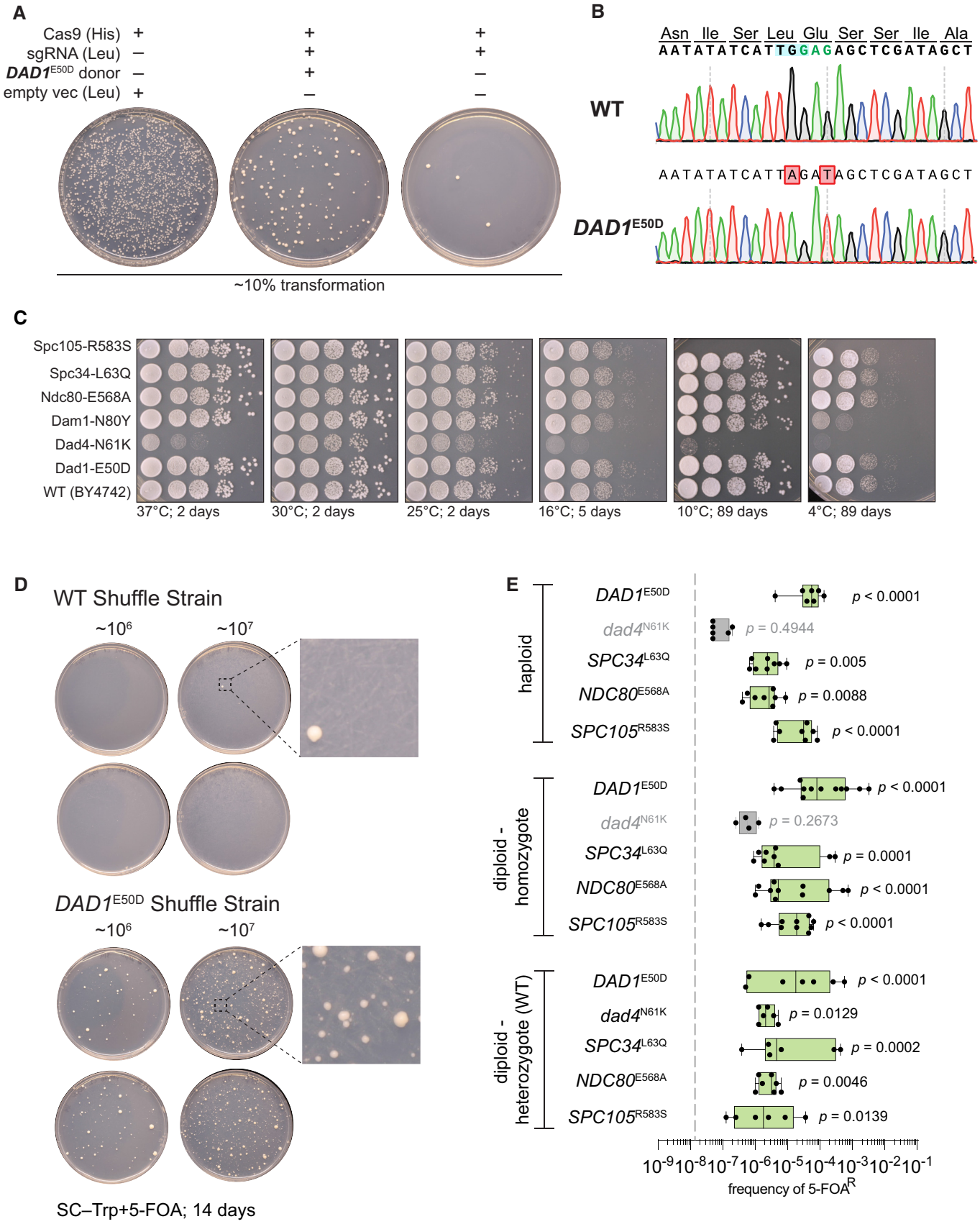

Figure EV2.

Figure EV3. Chromosome size alone does not explain the frequency of aneuploidy in yeasts.

A Correlation matrix of features of centromeres and aneuploidy frequency. Only correlations with significance ($P < 0.05$) are shown. The number of *CEN*-like regions is taken from Lefrançois *et al* (2013) and the pericentromeric sizes are taken from Paldi *et al* (2020).

B Histogram of the number of aneuploidies per chromosome from this study and nine additional studies (see text). Inset shows a boxplot of the same data with paired t-test of the mean difference in aneuploid frequency between groups A and B. Each dot represents the observed number of aneuploids from our study and nine additional studies ($n = 80$ for each group), the central band represents the median, the box extends from the 25th to 75th percentile, and the whiskers represent the 95% confidence interval.

C Randomizations of the mean difference in aneuploidy occurrence between centromere paralog pairs. Left panel, schematic of the analysis. Briefly, we examined the mean difference in aneuploidy frequency between centromere paralog pairs (Group A—Group B, e.g., CEN1—CEN7) in our study and nine additional studies (Table EV3; Kao *et al*, 2010; McCulley & Petes, 2010; Selmecki *et al*, 2015; Gallone *et al*, 2016; Zhu *et al*, 2016; Jaffe *et al*, 2017; Duan *et al*, 2018; Peter *et al*, 2018; Sharp *et al*, 2018). Next, from these 70 paired aneuploid values (note, we excluded the comparison of pair CEN15-CEN13), we calculated the difference in aneuploidy occurrence between each group A and group B pairs. We then performed a paired t-test on the mean difference in aneuploid occurrence between group A and group B pairs ($t = 3.95$, $P = 0.0001846$). To evaluate how "extreme" the observed *t*-statistic is, we performed randomized allocations of the observed differences in aneuploid occurrence. Succinctly put, we randomly assigned the sign (− or +) to the differences between group A and B paralog pairs and then calculated *t*-statistics from 100,000 randomized such allocations. The randomizations yielded a distribution of *t*-statistics of the mean difference in aneuploid occurrence between pairs assuming the null hypothesis is true (i.e., there is no difference in aneuploid frequency between the two groups). Right panel: histogram of the *t*-statistics from 100,000 randomizations of the difference in aneuploid occurrence. The observed *t*-statistic is shown with a red dashed line ($P < 0.00004$).

D Comparison of linear regression models of aneuploid frequency explained by the indicated factors. Regression models were compared using the Akaike information criterion (AIC) method.

E Example predictions from linear regression models based on chromosome size with or without the centromere paralog information.

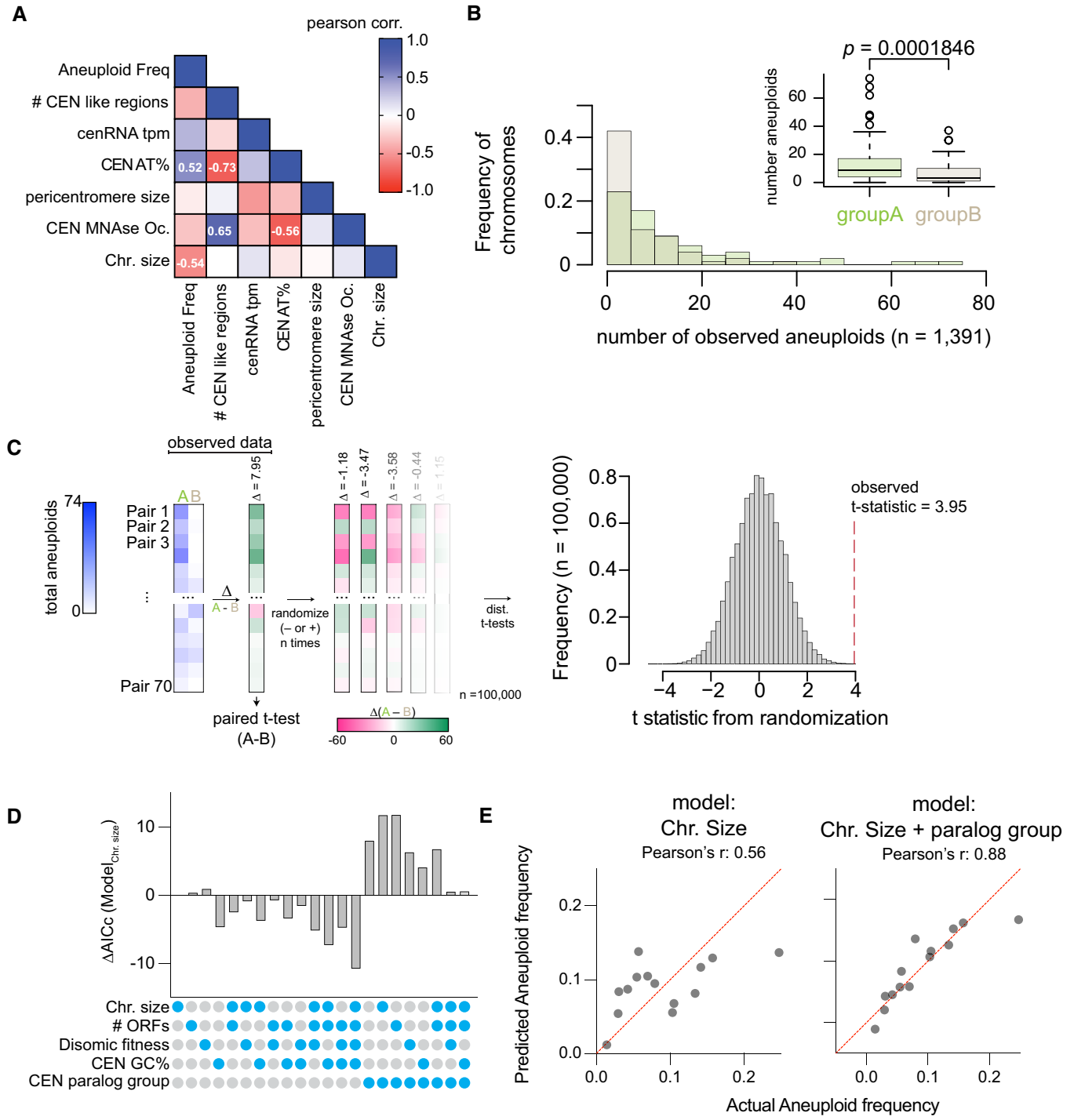

Figure EV3.

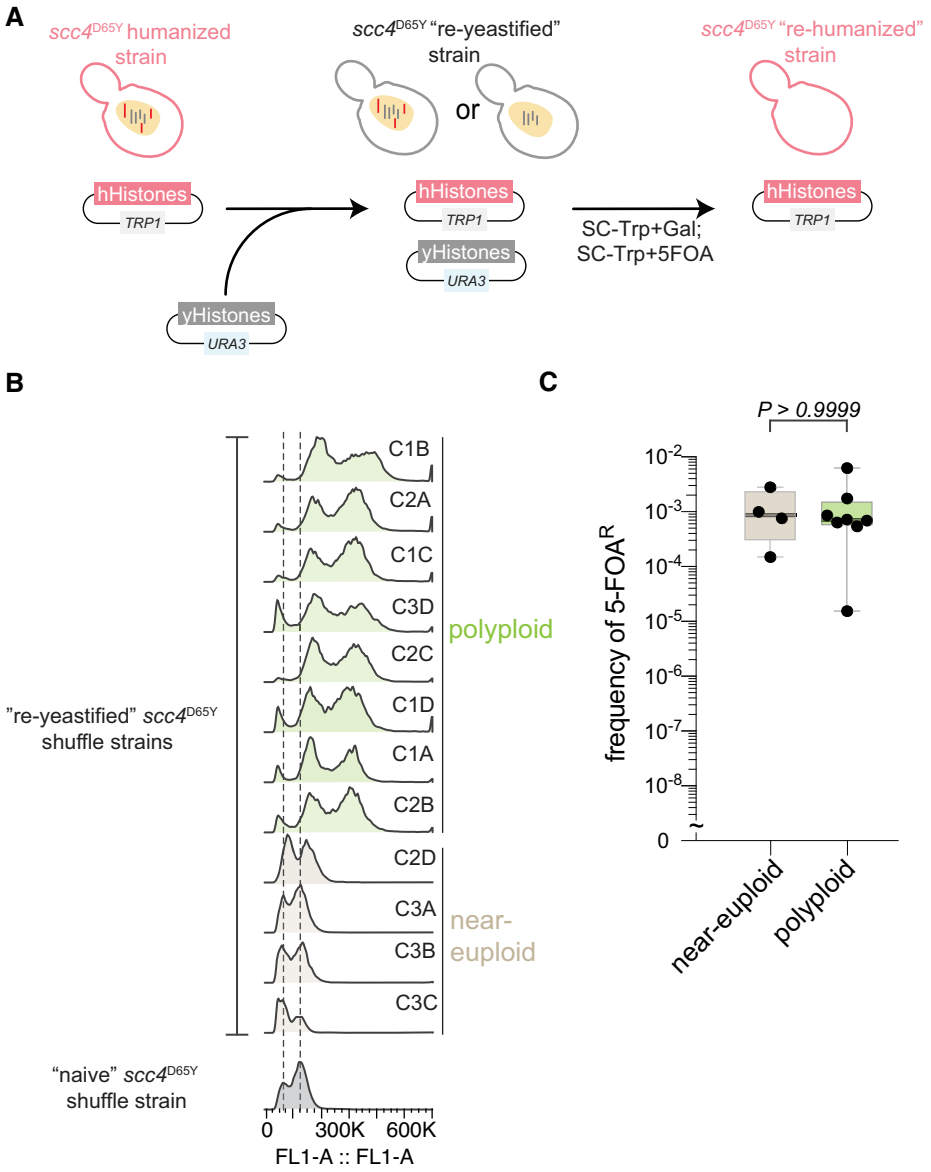

Figure EV4. Aneuploidy is non-adaptive for histone-humanization.

A Schematic of the re-yeastification process. First an already histone-humanized strain is transformed with the plasmid encoding all four yeast core histones, then is immediately re-humanized by counterselection of the same.

B Ploidy analysis using flow cytometry of the re-yeastified *scc4*^{D65Y} strains and the parental strain that has never had human histones.

C Frequency of 5–FOA^{R}-resistant colonies following histone humanization of the re-yeastified strains. Kruskal–Wallis test with Dunn's multiple corrections; test against the parent *scc4*^{D65Y} strain show that both euploid and polyploidy strains humanize at significantly higher rates, $P = 0.009$ and $P = 0.0034$, respectively. Each dot represents a biological replicate of the histone humanization assay ($n \geq 4$), the central band represents the median, the box extends from the 25th to 75th percentile, and the whiskers represent the minimum to maximum.

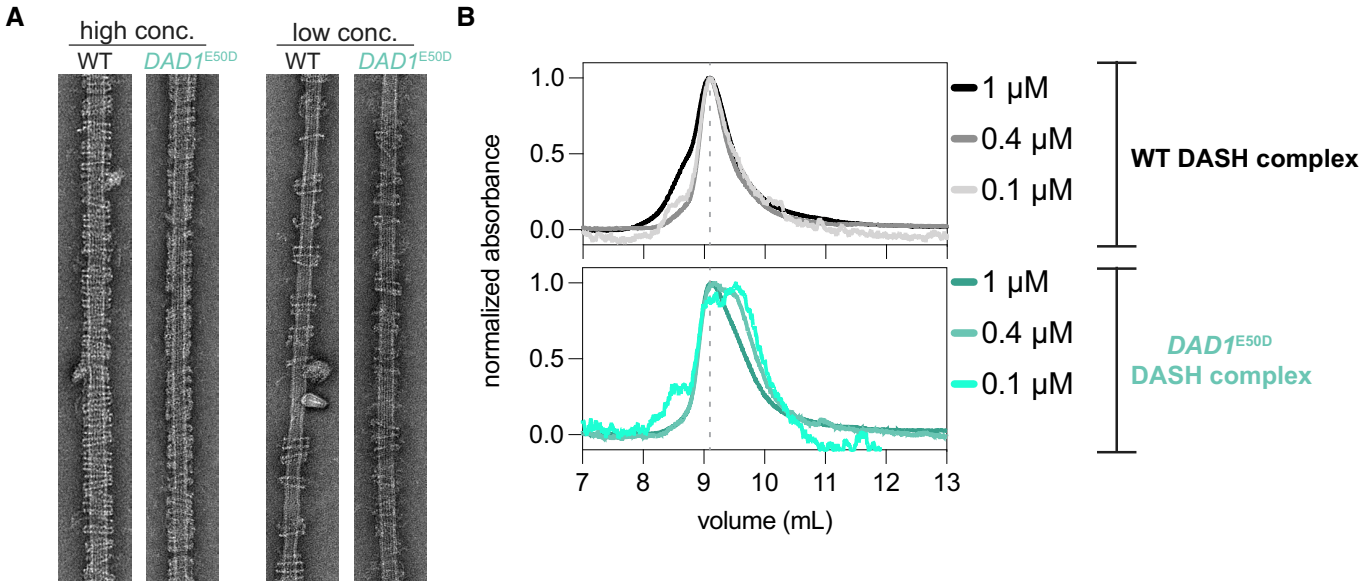

Figure EV5. *DAD1*^{E50D} disrupts DASH/Dam1c oligomerization and reduces its dimerization.

A Example EM images of DASH rings taken at low and high concentrations. High concentration > 25 nM complex and low concentration 11–16 nM complex. Microtubules are at a concentration of 20 nM tubulin dimer.

B Size exclusion chromatography of WT (upper graph) and mutant *DAD1*^{E50D} (lower graph) DASH complexes. Three dilutions of the DASH complex are shown. SEC analysis at lower concentrations of the mutant complex, but not for the WT complex, reveal the emergence of a second peak due to a species with a lower apparent molecular weight.